Feedback-dependent generalization

Jordan A. Taylor, Laura L. Hieber and Richard B. Ivry

J Neurophysiol 109:202-215, 2013. First published 10 October 2012;
doi: 10.1152/jn.00247.2012

Journal of Neurophysiology publishes original articles on the function of the nervous system. It is published 24 times a year (twice monthly) by the American Physiological Society, 9650 Rockville Pike, Bethesda MD 20814-3991. ESSN: 1522-1598. Visit our website at http://www.the-aps.org/.

J Neurophysiol 109: 202–215, 2013.
First published October 10, 2012; doi:10.1152/jn.00247.2012.

Feedback-dependent generalization

Jordan A. Taylor,[1] Laura L. Hieber,[2] and Richard B. Ivry[2,3]

[1]*Department of Psychology, Princeton University, Princeton, New Jersey;* [2]*Department of Psychology, University of California, Berkeley, California; and* [3]*Helen Wills Neuroscience Institute, University of California, Berkeley, California*

Submitted 23 March 2012; accepted in final form 7 October 2012

Taylor JA, Hieber LL, Ivry RB. Feedback-dependent generalization. *J Neurophysiol* 109: 202–215, 2013. First published October 10, 2012; doi:10.1152/jn.00247.2012.—Generalization provides a window into the representational changes that occur during motor learning. Neural network models have been integral in revealing how the neural representation constrains the extent of generalization. Specifically, two key features are thought to define the pattern of generalization. First, generalization is constrained by the properties of the underlying neural units; with directionally tuned units, the extent of generalization is limited by the width of the tuning functions. Second, error signals are used to update a sensorimotor map to align the desired and actual output, with a gradient-descent learning rule ensuring that the error produces changes in those units responsible for the error. In prior studies, task-specific effects in generalization have been attributed to differences in neural tuning functions. Here we ask whether differences in generalization functions may arise from task-specific error signals. We systematically varied visual error information in a visuomotor adaptation task and found that this manipulation led to qualitative differences in generalization. A neural network model suggests that these differences are the result of error feedback processing operating on a homogeneous and invariant set of tuning functions. Consistent with novel predictions derived from the model, increasing the number of training directions led to specific distortions of the generalization function. Taken together, the behavioral and modeling results offer a parsimonious account of generalization that is based on the utilization of feedback information to update a sensorimotor map with stable tuning functions.

generalization; modeling and simulation; motor adaptation; motor control; motor learning

GENERALIZATION HAS BEEN USED as a probe on the representational changes that occur during learning (Poggio and Bizzi 2004; Thoroughman and Shadmehr 2000). A common method to study generalization is to employ a visuomotor perturbation that introduces errors between a desired movement and the actual movement. Participants are trained with this perturbation in one movement direction or in a limited region of the workspace and then tested with movements in other directions (Ghahramani et al. 1996; Krakauer et al. 2000; Pine et al. 1996). How the system generalizes from a limited training set can provide insight into computational principles underlying sensorimotor learning and control (Poggio and Bizzi 2004), such as relating the pattern of generalization to the neural tuning properties (Donchin et al. 2003; Poggio and Bizzi 2004; Thoroughman and Taylor 2005).

A range of visuomotor perturbations have been employed in studies of generalization. Somewhat surprisingly, the results have failed to provide a consistent picture of generalization. Visuomotor rotations in which an angular displacement is imposed between the position of the unseen hand and a visual cursor results in rather narrow generalization (Krakauer et al. 2000; Pine et al. 1996). Generalization is prominent for directions similar to the trained direction but falls off sharply as the probed directions differ from the trained direction (Krakauer et al. 2000; Pine et al. 1996; Tanaka et al. 2009). Visuomotor gain adaptation, in which the amplitude between hand movement and cursor displacement is altered, also produces maximal generalization near the direction of training but exhibits considerable generalization for all directions of movement (Krakauer et al. 2000; Pearson et al. 2010; Vindras and Viviani 2002). Similarly, linear shifts of the visual input, the type of perturbation created by prism glasses, generalize relatively broadly across the workspace (Ghahramani et al. 1996). Dynamic perturbations such as those employed in studies using force field environments have also been used to study generalization. The results from this work indicate that the pattern of generalization is dependent on the complexity of the perturbation (Donchin et al. 2003; Thoroughman and Shadmehr 2000; Thoroughman and Taylor 2005).

While certain features of generalization functions are similar across these studies (e.g., maximal generalization for movements most similar to the training set), the subtle differences have been the focus of considerable debate given their potential to reveal the representational changes that occur during sensorimotor learning. Two key features are thought to define the form of generalization. First, generalization will be constrained by the underlying units that control the movements. For example, if the units are directionally tuned neurons, generalization is constrained by the width of the tuning functions (Thoroughman and Shadmehr 2000). Second, errors are used to update the sensorimotor map, altering the weights between the tuned units and desired directions of movement (Pouget and Snyder 2000). Learning algorithms combine these two features to ensure that the error only modifies those units that were responsible for the error. As such, if the underlying units represent movement space broadly, generalization will be broad because many units are affected by the error signal (Thoroughman and Shadmehr 2000). In contrast, if the units represent space narrowly, then generalization will be limited given that units tuned to distant directions are unaffected by the error. Thus patterns of generalization have been used to identify computational properties of the motor control system (Ghahramani et al. 1996; Poggio and Bizzi 2004; Pouget and Snyder 2000; Thoroughman and Shadmehr 2000).

As described above, generalization studies have been exploited to explore the tuning properties of motor control elements (Thoroughman and Shadmehr 2000). For example, Thoroughman and Taylor (2005) trained participants to move

Address for reprint requests and other correspondence: J. A. Taylor, Dept. of Psychology, Princeton Univ., 3-S-13 Green Hall, Princeton, NJ 08544 (e-mail: jordanat@princeton.edu).

in force field environments with varying degrees of dynamical complexity. While learning was reasonably similar across conditions, the generalization functions were quite different. To account for these differences, two hypotheses were suggested. One centered on the idea that there exists a heterogeneous population of tuning functions with a range of widths; by this account, the relevant set of tuning functions for learning will vary with task complexity. The second hypothesis centered on the idea that the width of the tuning functions is altered with training, and that the extent of these changes will vary with task complexity. While experimental studies testing these hypotheses have not been reported, both hypotheses necessitate that the tuning function of the neural units must be different to learn different environmental complexities.

A few studies have asked how error signals may contribute to task-dependent effects on generalization. Depending on the form of a visuomotor perturbation (e.g., rotational or translational), generalization can either be expressed in a Cartesian reference frame or rotational (Ghahramani et al. 1996; Krakauer et al. 2000). Moreover, the strength of generalization is influenced by the availability of error information: Adaptation (Rapp and Heuer 2011) and generalization are stronger when feedback is continuously available during the reach compared with when it is provided only at the end of movement (Hinder et al. 2008; Shabbott and Sainburg 2010). Although the consequences of these error manipulations have not been examined in a formal manner, these results suggest that task-dependent differences in generalization may reflect variation in the availability of error information for adapting the sensorimotor system. Specifically, a change in error information may influence generalization because more states are subject to error-based modification during training.

The present study was designed to provide a systematic analysis of the influence of error information on generalization. In the main experiment, participants were trained on a visuomotor rotation task, with the training phase limited to a single direction of movement, followed by generalization to untrained, distant locations. Between groups, we manipulated the form of the visual feedback, providing either endpoint or online feedback and within the latter varying whether or not the movement had to terminate in the target location. While the groups displayed similar learning curves during the training period, they exhibited strikingly different generalization patterns. Building on previous work (Pearson et al. 2010; Tanaka et al. 2009; Thoroughman and Shadmehr 2000; Thoroughman and Taylor 2005), we employed a radial basis function network to simulate the patterns of generalization. We show that qualitatively different patterns of generalization can be produced in such a network because of variation in the error signal, even if the underlying tuning functions remain invariant. A second experiment was conducted in which we extended the range of training directions to test a novel prediction derived from the model.

MATERIALS AND METHODS

Participants and Experimental Apparatus

Sixty young adults (35 women/25 men, age 22 ± 7 yr) were recruited from the research participation pool maintained by the Department of Psychology at the University of California, Berkeley. All participants were right-handed, as verified with the Edinburgh handedness inventory (Oldfield 1971), and received class credit. The experimental protocol was approved by the University of California's Institutional Review Board, and all participants gave informed consent.

Participants made center-out, horizontal reaching movements to visually displayed targets, sliding their right hand across a digitizing tablet while holding onto a digitizing pen (Intuous 3; Wacom, Vancouver, WA). Movement trajectories were sampled at 100 Hz. The stimuli and feedback cursor were displayed on a 15-in., 1,280 × 1,024-pixel-resolution LCD computer monitor (Dell, Dallas, TX) horizontally mounted 25.4 cm above the table. Since the monitor occluded vision of the hand, visual feedback was in the form of a small circular cursor (3.5 mm).

Experiment 1

Forty participants were assigned to one of four experimental groups (Fig. 1), with ten participants per group. For all groups, the trial started with the participant moving his or her hand such that the feedback cursor was positioned in a starting circle (5-mm diameter). After 1 s at this position, a green target (7-mm-diameter dot) appeared on a blue ring (7 cm in radial distance from the starting circle). The target could appear in one of eight locations (0°, 45°, 90°, 135°, 180°, −135°, −90°, −45°). The participants were instructed to make a fast reaching movement to the target.

For the endpoint-feedback (ENDPOINT) group, participants only received endpoint feedback of the movement (knowledge of results). These participants were instructed to make a fast reaching movement, attempting to slice through the target. The feedback cursor disappeared when the participant's hand exited the starting circle. When the participant's hand had moved 7 cm, a red cursor (3.5 mm) appeared at the corresponding position (veridical or rotated) on the blue ring and remained visible for 1 s. For the online-feedback (ONLINE) group, feedback of hand position was provided during the entire outbound portion of the movement. When the radial amplitude reached 7 cm, the white cursor changed to red and remained posi-

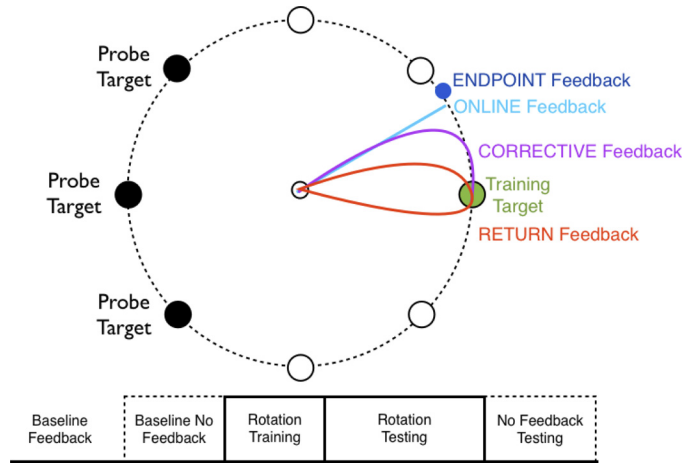

Fig. 1. Different forms of visual feedback for a center-out reaching task workspace. There were 8 target locations. Participants practiced reaching to all locations in the baseline blocks. During the training block, participants only moved to the target at 0° (green target) and a 30° rotation was applied to the cursor. During the test block, participants reached to the training location (with feedback) and the 3 probe locations (black, no feedback). Generalization to all locations was tested in a no-feedback block at the end of training. A ring connecting the target locations was visible during the reaches. The trial ended for the ENDPOINT and ONLINE groups when the movement intersected this ring, with feedback limited to the endpoint for the former (blue) and visible until the hand intersected the target ring for the latter (cyan). The corrective feedback group (purple) had online feedback and was required to hit the target to end the movement. The return group (red) had online feedback during reaches to the target and during the return movement to the starting position.

tioned on the blue ring for 1 s (as with the ENDPOINT group). Participants in the ENDPOINT and ONLINE groups were instructed that the goal was to have the red feedback cursor be positioned as close to the target as possible. In contrast, participants in the corrective-feedback (CORRECTIVE) group received online feedback and were required to bring the white cursor within the target circle to end the trial. When any part of the cursor overlapped the target, the feedback color changed to red and remained fixed in place for 1 s.

Participants in all three groups were trained to reach the blue ring within 300–500 ms. If this criterion was met, a pleasant "ding" sound was played; otherwise an unpleasant "buzz" sound was played. In addition, if the movement time criterion was met and any part of the feedback cursor overlapped the target, the participant received 1 point. Note that CORRECTIVE participants always had to hit the target; thus their bonus was solely dependent on the temporal criterion. The points were tallied throughout the experiment, with the sum displayed at the end of each block.

After the 1-s endpoint feedback delay, participants in the ENDPOINT, ONLINE, and CORRECTIVE groups were required to reposition the hand in the starting circle. The participant was guided to the starting position by a white ring with a diameter equal to the distance of the hand from the starting position. By the hand moving toward the starting circle, this ring became progressively smaller. When the hand was within 1 cm of the starting circle, the ring was transformed into the white feedback cursor, allowing the participant to position the hand within the starting circle.

Participants in the return-feedback (RETURN) group had continuous online feedback of the cursor during both the out and back phases of the movement. They were instructed to reach the target within 300–500 ms, with the feedback cursor changing from white to red when it overlapped any part of the target. The feedback cursor remained fixed at this position for 1 s, before changing back to white. Participants were instructed to keep their hand still during the 1-s feedback interval. If the participant moved >1 cm from the terminal position, a double buzz sound was played to remind the participant that he or she should remain still during the feedback interval. Once the feedback cursor turned white, the participant was instructed to return to the starting circle. There was no temporal criterion for the return movement, but online feedback was available at all times.

All participants made a total of 266 movements, divided into a series of blocks (Fig. 1). The groups were initially trained with their assigned feedback format for 64 baseline trials, with each of the 8 target locations presented 8 times. Feedback was veridical during this phase, allowing the participants to become accustomed to the reaching task and learn the desired movement speed. Participants then made another 32 baseline movements, 4 to each target. On half of the trials, feedback was presented. On the other half of the trials, the feedback went blank at the start of the movement. Participants were not informed whether a trial included feedback or not, only discovering this once the movement started. On no-feedback trials, the participants were instructed to just reach through the visible blue ring, attempting to maintain their adopted movement velocity. For all groups, the contracting white ring was used to guide the hand back to the starting position after each no-feedback trial. This block was included to provide the participants with experience at moving in the absence of feedback.

The two baseline blocks were followed by a 40-trial rotation block. For this block, all of the reaches were to a single "training" location at 0°. Feedback of hand position (either online or endpoint, depending on the group) was rotated 30° counterclockwise (CCW). The rotation block was followed by a test block in which reaches to the training location were intermixed with reaches to three probe locations (135°, 180°, and −135°). Rotated visual feedback was only provided on trials in which the target appeared at the training location; no feedback was given when the movements were at the probe locations. The test block consisted of 90 reaches, 45 to the training location and 15 to each of the three probe locations. The target sequence was pseudorandomly distributed such that, for every four movements, two were to the training location and two were to probe locations. We restricted the probe locations to those that were most distant from the training location since these are most informative for assessing the reference frame of generalization (see below).

The experiment concluded with a final no-feedback block composed of 40 trials, 5 to each of the 8 target locations. Visual feedback was absent during this entire block, providing an assessment of generalization at all locations in the absence of (re)learning.

The experimental session lasted ~40 min.

Experiment 2

Twenty participants were assigned to one of two experimental groups, the ENDPOINT-TWO and RETURN-TWO groups, with ten participants per group. The baseline blocks were the same as in *experiment 1*. In the rotation block, participants were trained with the rotation at two locations (0° and −45°), with 20 trials at each location. In the test block, reaches to these two locations were pseudorandomly interspersed with trials to the three probe locations. After the rotation block, participants experienced the no-feedback block composed of 40 trials, 5 to each of the 8 target locations, to assess generalization at all target locations.

For the ENDPOINT-TWO group, participants received only endpoint feedback of the movement, similar to the ENDPOINT group from *experiment 1*. For the RETURN-TWO group, participants received online feedback throughout the entire movement, similar to the RETURN group from *experiment 1*. Feedback was provided at all locations during the baseline blocks and only for movements to the two training locations in the rotation and test blocks.

Data Analysis

Kinematic and statistical analyses were performed with MATLAB (MathWorks, Natick, MA). To assess adaptation and generalization, we focused on the initial heading angle of the hand. Each movement trajectory, regardless of the actual target location, was rotated to a common axis with the target location at 0°. A straight line was connected between referent points 1 cm and 3 cm along the trajectory, and we computed the angle between this line and the 0° reference line. With this convention, positive angles indicate a positive deviation along the *y*-axis and negative angles indicate a negative deviation along this axis. To compute the rate of adaptation, we fit the time series of heading angles in the rotation block with an exponential function using the simplex method (Nelder and Mead 1965). The adaptation rate and final asymptotic values are reported in RESULTS.

We also computed the curvature of each movement in order to assess the presence and form of corrective movements. Movement curvature was defined as the total absolute curvature in Cartesian coordinates:

$$C = \frac{\left| v_x a_y - v_y a_x \right|}{\left(v_x^2 + v_y^2 \right)^{3/2}}$$

where v_x and v_y are the *x*- and *y*-components of velocity and a_x and a_y are the *x*- and *y*-components of acceleration. Velocity and acceleration were computed with a 4th-order Savitsky-Golay filter. This filter introduces less noise than basic difference differentiation (Savitzky and Golay 1964; Smith et al. 2000).

Movement onset was defined by identifying the maximum velocity and scanning the kinematic record backward to determine the last sign reversal in the velocity record. For the ONLINE and ENDPOINT groups, movement time was defined as the interval between movement onset and the time at which the hand crossed the target ring. For the CORRECTIVE and RETURN groups, movement time was quantified as the interval between movement onset and the time at which any part of the feedback cursor overlapped the target circle.

We report the mean and the 95% confidence interval of the mean for all dependent variables subjected to statistical evaluation.

Modeling

We simulated generalization functions, using a radial basis function network (Tanaka et al. 2009). Identical basis units were employed for all four groups, with the units defined by wrapped Gaussian functions that encoded hand-centered reach directions:

$$g_n^i(\theta_\pi^{\text{desired}}) = a + \frac{1}{\sqrt{2\pi\sigma^2}} \sum_{k=2\pi}^{2\pi} \exp\left(\frac{-(\theta_n^{\text{desired}} - \theta^i)^2 + k}{2\sigma^2} \right) \quad (1)$$

The activity for unit i on trial n is dependent on the difference between that unit's preferred direction (θ^i) and the desired target direction ($\theta_n^{\text{desired}}$). Each unit in the network has the same tuning breadth (σ) and baseline activity (a). We employed a wrapped Gaussian function because it equates angles separated by 2π (e.g., $0 = 2\pi$).

The population-based vector for the desired reach direction ($\vec{r}_n^{\text{desired}}$) is given by the sum of the weighted (w) activity of each unit (inner product):

$$\vec{r}_n^{\text{desired}} = \sum_{i=0}^{2\pi} \vec{w}^i g^i\left(\theta_n^{\text{desired}}\right) = WG\left(\theta_n^{\text{desired}}\right) \quad (2)$$

We used a gradient-descent learning rule to change the weights (w), where each weight was adjusted based upon the degree of its activity and the observed error.

Models of error-based learning need to consider when the error is generated. In many studies of visuomotor adaptation, the error is defined at a single point in time—for example, when the movement amplitude equals the target distance or at the terminal location of the movement when participants make a single, outbound reach (Izawa and Shadmehr 2011; Tseng et al. 2007). At the other extreme, feedback information, at least when online feedback is available, could provide a continuous error signal. We opted to employ an intermediate approach, considering two, discrete error signals, one used to update the weights based on errors observed during the outbound phase of the movement and a second used to update the weights on the corrective, or return phase of the movement (see below). For the ENDPOINT and ONLINE groups, only the outbound error was used to update the weights (*Eq. 3*). For the CORRECTIVE and RETURN groups, both the outbound (*Eq. 3*) and corrective/return (*Eq. 4*) errors were used to update the weights. The two error signals were modulated by their own learning rate η:

$$\Delta W_{\text{outbound}} = -\eta_1 G\left(\theta_n^{\text{desired}}\right) e_{\text{outbound}} \quad (3)$$

$$\Delta W_{\text{correction/return}} = -\eta_2 G\left(\theta_n^{\text{correction/return}}\right) e_{\text{correction/return}} \quad (4)$$

The error (*Eq. 6*) for the outbound portion of the movement was defined as the difference between the desired movement direction (*Eq. 2*) and the target direction (*Eq. 5*) at the onset of the movement:

$$\vec{r}_n^{\text{target}} = \begin{bmatrix} \cos\left(\theta_n^{\text{target}}\right) \\ \sin\left(\theta_n^{\text{target}}\right) \end{bmatrix} \quad (5)$$

$$e_{\text{outbound}} = R\vec{r}_n^{\text{desired}} - \vec{r}_n^{\text{target}} \quad (6)$$

To simulate the rotation, the desired reach vector was rotated by a rotation matrix, where $\varphi = 30°$:

$$R = \begin{bmatrix} \cos(\phi) & \sin(\phi) \\ -\sin(\phi) & \cos(\phi) \end{bmatrix} \quad (7)$$

The error for the corrective portion of the movement was defined similar to the outbound error (*Eq. 9*), but here the desired movement direction (*Eq. 2*) was based on required direction for the correction to the target location or the return movement to the home position (*Eq. 8*):

$$\vec{r}_n^{\text{correction/return}} = \begin{bmatrix} \cos\left(\theta_n^{\text{correction/return}}\right) \\ \sin\left(\theta_n^{\text{correction/return}}\right) \end{bmatrix} \quad (8)$$

$$e_{\text{correction/return}} = R\vec{r}_n^{\text{desired}} - \vec{r}_n^{\text{correction/return}} \quad (9)$$

For the RETURN group, the $\theta_n^{\text{correction/return}}$ direction was set to 180°. For the CORRECTIVE group, different directions were simulated to determine the direction of the correction that resulted in the appropriate pattern of generalization (see RESULTS). Note that only a single time point was used for each error term. In reality, there is a continuous error signal. While it is unknown whether control processes use a continuous process, our choice here was motivated by two considerations. First, using discrete samples greatly simplifies the modeling work, especially since a continuous error signal requires making an assumption about the desired trajectory. Second, our main interest here is to test of a proof of concept regarding the potential impact of different feedback signals on generalization. As such, the inclusion of two discrete samples, one for the initial, outbound phase of the movement and the other for the corrective/return phase, should suffice. It is important to note that our model does not represent a time series of heading directions but rather only two distinct time points for the heading direction, one time point for the heading direction of the outbound phase and one for the corrective/return phase. To simulate the outbound phase, the units generate a population vector specifying a single heading direction for the entire outbound phase of the movement. The difference between this heading angle and the target angle specified the outbound error. This error was applied to all of the units; based upon the gradient learning rule (*Eq. 3*), only the weights associated with the units that were highly activated would be significantly altered. To simulate the corrective/return phase, a population vector is generated to specify the heading direction for the corrective/return phase of the movement. The difference between this heading angle and the angle of correction to the target or start position specified the corrective/return error. This error was then applied to all of the units in a similar manner as for the outbound error. Thus there are only two time points for updating throughout the movement.

To generate trajectories for plotting purposes, the two heading directions can be multiplied by a time vector to mimic actual movement time. Note that we did not directly compare observed trajectories with model-produced trajectories because our fitting procedure only compares the observed and predicted heading angles (see below). While the model could be set to use any number of time points and thus generate full trajectories, this becomes computationally intractable, leading us to adopt the two-time point simplification. A similar simplification has been used in previous studies, but only using one time point to update movements (Tanaka et al. 2009; Throughman and Shadmehr 2000; Thoroughman and Taylor 2005).

The best-fitting parameters of the model were found by a nonlinear least-squares fitting procedure based on the Gauss-Newton method. This procedure was set up to minimize the averaged heading angle for each group for the first movement to each target during the no-feedback block. Heading angle was calculated as the difference between a line from the start position to the target location and a line with endpoints based on hand position, 1 and 3 cm into the movement. We constrained parameters a, σ, and η_{outbound} to take on a single value for all four groups. Parameters $\theta_n^{\text{correction/return}}$ and $\eta_n^{\text{correction/return}}$ were allowed to differ for the CORRECTIVE and RETURN groups. For *experiment 2*, the parameter values for the ENDPOINT and RETURN groups were held constant for the model simulations. The model was trained nearly identically to *experiment 1*, except that there were two training locations during the rotation block and the test block.

RESULTS

Experiment 1

Kinematic differences between feedback groups prior to rotation training. We first sought to determine how feedback might alter movement kinematics in the absence of a rotation. As described above, participants in the CORRECTIVE and

Table 1. *Temporal, kinematic, and learning measures for the four groups*

Groups	Baseline FB	Baseline No FB	Final Value	Rate
Movement time, s				
ENDPOINT	0.37 ± 0.02	0.38 ± 0.03		
ONLINE	0.39 ± 0.04	0.39 ± 0.04		
CORRECTIVE	0.42 ± 0.05	0.39 ± 0.05		
RETURN	0.50 ± 0.07	0.43 ± 0.02		
Intertrial interval, s				
ENDPOINT	2.13 ± 0.44	1.94 ± 0.35		
ONLINE	1.93 ± 0.23	2.04 ± 0.24		
CORRECTIVE	2.04 ± 0.39	1.81 ± 0.23		
RETURN	2.44 ± 0.40	2.10 ± 0.25		
Total curvature, cm^2				
ENDPOINT	15.5 ± 6.97	12.2 ± 8.20		
ONLINE	3.12 ± 1.60	5.69 ± 5.47		
CORRECTIVE	40.9 ± 21.9	48.9 ± 82.2		
RETURN	39.8 ± 32.5	22.7 ± 20.4		
Heading angle, °				
ENDPOINT	0.21 ± 0.82	−0.06 ± 1.22		
ONLINE	1.23 ± 1.75	0.84 ± 1.78		
CORRECTIVE	0.67 ± 1.24	0.99 ± 1.07		
RETURN	1.96 ± 1.13	1.45 ± 0.99		
Rotation training				
ENDPOINT			−25.8 ± 3.04	3.98 ± 3.24
ONLINE			−25.3 ± 1.68	2.84 ± 1.37
CORRECTIVE			−23.0 ± 1.65	2.35 ± 0.97
RETURN			−24.2 ± 1.64	2.07 ± 0.76

Means and 95% confidence intervals of the mean are reported. Movement time, intertrial interval, movement curvature, and heading angle are shown for each group during the baseline phase, with and without endpoint feedback (FB). Learning rate and final asymptotic value are based on exponential fit of the adaptation curve in the rotation training block.

RETURN groups were required to hit the target. In contrast, for participants in the ENDPOINT and ONLINE groups the trial ended when the hand passed the target ring. Since the second baseline block included reaches to all eight targets, with and without feedback, we focused on these data to assess the effect of feedback on movement time and curvature.

Average movement times were within the 300–500 ms time window for both feedback-present and feedback-absent trials in all four groups (Table 1). A two-way ANOVA revealed no effect of feedback (present/absent) ($F_{1,36} = 2.17$, $P = 0.15$). However, there was a significant effect of group ($F_{3,36} = 6.85$, $P = 0.004$). Movement times were progressively longer as the amount of feedback increased, becoming especially pronounced in the groups that were required to hit the target. A similar pattern was observed in the evaluation of movement curvature: The degree of movement curvature was similar for feedback-present and feedback-absent trials ($F_{1,36} = 0.06$, $P = 0.98$), while the effect of group was reliable ($F_{3,36} = 2.68$, $P = 0.05$). Participants in the CORRECTIVE and RETURN groups had more movement curvature, presumably due to the fact that these participants had to make corrective, secondary movements when the initial trajectory failed to terminate at the target. Consistent with this assumption, the curvature differences appear to be limited to the latter phase of the movements since the group effect was not significant in an analysis of heading angles ($F_{1,36} = 2.17$, $P = 0.10$).

An additional comparison of baseline performance was restricted to the data from the RETURN group. For this group, the feedback cursor was visible during both the out and back phases of the movement on the feedback trials. On the no-feedback trials, the return movement was guided by the contracting ring. Despite this pronounced methodological difference, the duration of the return movement was similar for the two groups ($t_9 = 1.59$, $P = 0.15$). Indeed, when all four groups were considered, there was no difference in the duration of the return movement between groups ($F_{3,36} = 1.08$, $P = 0.37$).

Kinematic differences during and after rotation training. After baseline training, the rotation block was introduced. A 30° CCW rotation was imposed for 40 movements, all of which were made to a single target at 0°. Rapid adaptation was observed in all four groups, with the final heading angles falling short of the full rotation (Fig. 2). An exponential function was fit to the time series of heading angles for each participant in each group. There was no difference in final degree of adaptation ($F_{1,36} = 1.33$, $P = 0.28$) or adaptation rate ($F_{1,36} = 0.79$, $P = 0.51$), suggesting that differences in feedback conditions did not significantly affect the course of adaptation (Table 1).

After this short adaptation phase, participants were tested on the test block in which three distant probe locations (135°, 180°, −135°) were intermixed with the training location (0°). Feedback was limited to the training location. Changes from baseline in the heading angles to the probe locations provide a signature of generalization (Fig. 3). These data reveal subtle but important differences between the groups in the pattern of generalization at the probe locations. Main effects were reliable for the factors group ($F_{3,36} = 6.55$, $P < 0.001$) and probe location ($F_{2,72} = 6.22$, $P = 0.003$). The average trajectories to the probe targets in the ENDPOINT and ONLINE groups were biased downward in the workspace, a change that is opposite to the rotational direction observed at the trained location. In contrast, participants in the RETURN group showed generalization consistent with the direction of the rotation at the

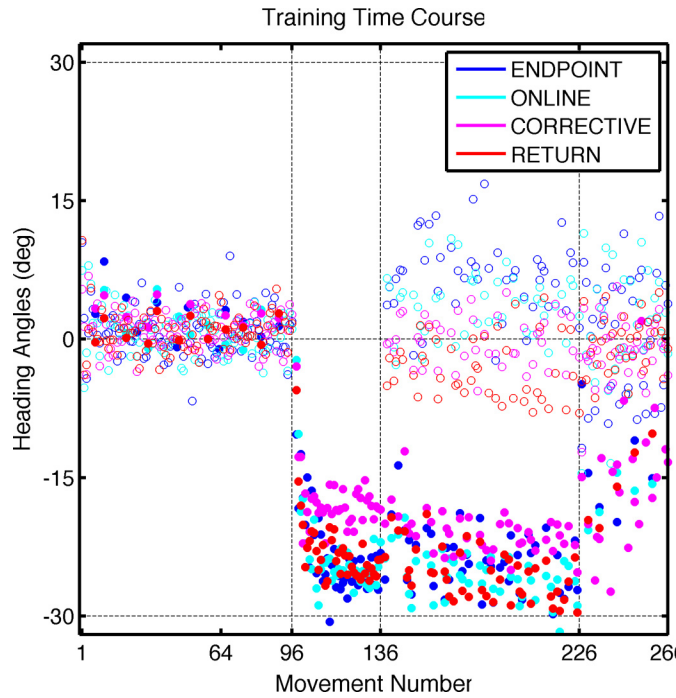

Fig. 2. Heading angle relative to target direction during baseline (*trials 1–96*), rotation (*97–136*), test (*137–226*), and no-feedback (*227–266*) blocks. Colors correspond to the 4 groups: ENDPOINT (blue), ONLINE (cyan), CORRECTIVE (purple), RETURN (red). Movements to the training target location are filled circles, and movements to the other locations are open circles.

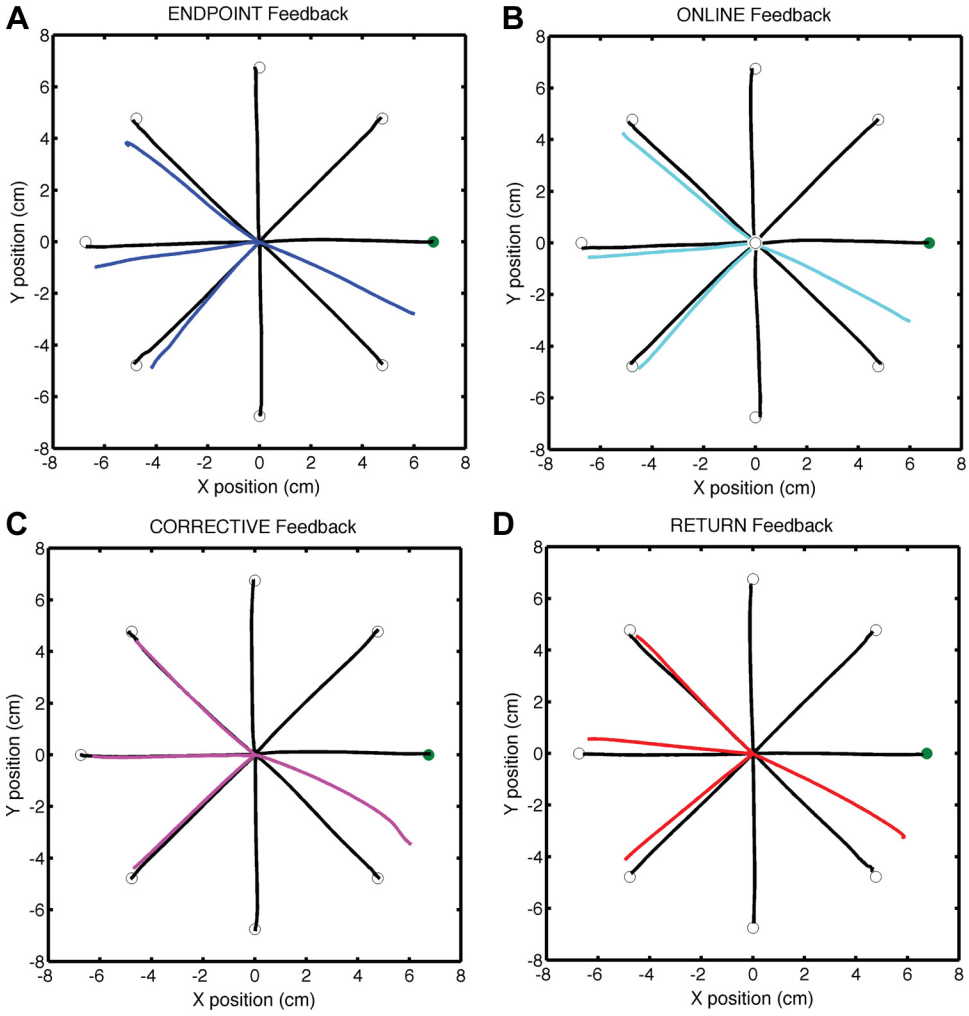

Fig. 3. Hand trajectories during the baseline block (black) and test block for the 4 groups: ENDPOINT (blue, *A*), ONLINE (cyan, *B*), CORRECTIVE (purple, *C*), RETURN (red, *D*). During the baseline block, feedback was provided at all locations. During the test block, feedback was provided on trials in which the target appeared at the training location. No feedback was provided on trials in which the target appeared at probe locations.

trained location. Across all four groups, generalization was larger at the 135° location compared with the other two locations. The group × probe location interaction was not significant ($F_{1,9} = 0.49$, $P = 0.81$). To determine whether these results may be driven, at least in part, by differential group biases in the second baseline block (where feedback and no-feedback trials were interleaved), we subtracted the average heading angle in the baseline block from the average heading angle in the test block for each target location. Similar to the uncorrected analysis, the effects of group ($F_{3,36} = 6.67$, $P = 0.004$) and probe location ($F_{2,72} = 4.77$, $P = 0.01$) were reliable after this correction, and the interaction was not significant ($F_{1,9} = 0.47$, $P = 0.83$).

Figure 4 displays the group means of the heading angles for the training location and probe locations. For the latter, we averaged across the three probe locations, given that the interaction term was not reliable and the direction of the generalization was internally consistent within each group. While all four groups showed similar changes in heading angle at the trained location, reflecting consistent adaptation, these summary data make clear the qualitative differences in generalization between the groups. The mean heading angles are in the opposite direction of the rotation for the two groups that were not required to hit the target (ENDPOINT and ONLINE). In contrast, the heading angle was in the direction of the rotation for the group that had feedback during the outbound and return phases of the movement (RETURN). As can be seen in the individual data in Fig. 4, there was little overlap in the generalization values between the groups.

During the no-feedback block, feedback was never presented and movements were made to all eight locations, allowing a probe on full generalization in the absence of error-driven learning. Figure 5 shows the average trajectories across participants, based on the first movement to each target during the no-feedback block. These trajectories were used to generate the generalization functions depicted in Fig. 8, with which the model was trained to fit. All four groups show similar generalization for targets near the training location (for locations 45° and −45°: group $F_{3,36} = 1.01$, $P < 0.39$; location $F_{1,36} = 0.01$, $P < 0.97$; interaction $F_{1,9} = 0.26$, $P < 0.85$). No generalization was observed at the vertical locations (90° and −90°: group $F_{3,36} = 0.06$, $P < 0.98$; location $F_{1,36} = 2.04$, $P < 0.16$; interaction $F_{1,9} = 0.79$, $P < 0.50$). For targets far from the training location, the no-feedback block results were similar to those observed in the test block, although the location effect was no longer significant (locations 135°, 180°, and −135°: group $F_{3,36} = 7.93$, $P < 0.0001$; location $F_{2,72} = 2.03$, $P < 0.14$; interaction $F_{1,9} = 0.38$, $P < 0.88$). We expected that generalization would be somewhat attenuated during the no-feedback

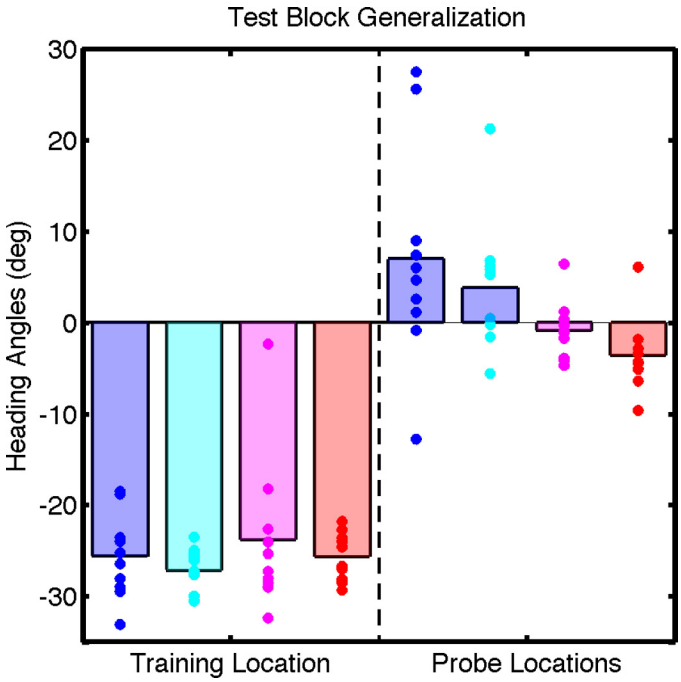

Fig. 4. Group-averaged heading angles (bars) relative to target direction for movements to the training and probe locations in the rotation block. Dots indicate individual participant values. Colors correspond to the 4 groups: ENDPOINT (blue), ONLINE (cyan), CORRECTIVE (purple), RETURN (red).

block given that there should be decay of adaptation with repeated movements without visual feedback.

Modeling. The radial basis function model (*Eqs. 1–9*) was used to simulate reaches during the baseline, rotation, test, and initial cycle of the no-feedback blocks. The parameters of the model were fit with a nonlinear least-squares approach, minimizing the average target error for each of the four groups during the first cycle of the no-feedback block. The model was initialized with randomized weights and trained for 96 movements, reaching to each target 12 times in the absence of a rotation. A separate weight matrix was used for each group; thus the weight matrices could differ at the start of the rotation training block. The error signal(s) were used to adjust the weight matrix, and by the end of the simulated movements in the baseline block the model was successful in reaching to each target with essentially no error (see Fig. 7). Note that while having different randomized weights, the models for the ENDPOINT and ONLINE group conditions converged because they are trained with the same outbound error and are not influenced by the corrective/return error term.

After the baseline block, the rotation was imposed for 40 trials, with all reaches limited to the training direction (0°). The model rapidly learned to adjust the heading angle to compensate for the rotation (Fig. 6). To simulate the test block, the rotation remained in place on trials in which the target appeared at the training location and the observed errors were used to update the weight matrix. Updates were not made after reaches to the probe locations since feedback was withheld on these trials. After the test block, the weight matrix was fixed and movements to each target were simulated to assess generalization at all target locations (1 cycle of the no-feedback block). Thus the model simulated the time series of reaches throughout every block, including the rotation and test block, as well during the first epicycle of the washout block.

By the end of this simulated training, the model's trajectories for the ENDPOINT and ONLINE conditions are identical since they use the same error, and closely match the hand trajectories for each group (Fig. 7). The generalization function for these groups provides an excellent match to the data (Fig. 8; Table 2). Significant generalization is observed at +45°/−45°, the targets near the training direction, and the pattern here is very similar across the four groups. Little generalization is observed at +90°/−90°. Generalization at these locations is primarily driven by the width of the basis function. The estimated value of this parameter (σ) was 16°, a value that is slightly narrower than previously estimated (Tanaka et al. 2009).

Generalization is not only driven by the width of the neural tuning function but also dependent on baseline activity of the simulated units (Ingram et al. 2011; Thoroughman and Taylor 2005). The estimated baseline activity was quite small (a = 0.04). Nonetheless, this small level of activity was sufficient to produce some degree of generalization at all locations. Importantly, the positive baseline activity produces generalization in a direction consistent with a Cartesian representation of the error, not in a rotational frame of reference. Thus the positive baseline activity produces the downward generalization at the probe locations for the ENDPOINT and ONLINE conditions (Fig. 7).

The positive baseline activity will also produce downward generalization effects for the CORRECTIVE and RETURN conditions. However, the generalization pattern for these groups is also influenced by the second error term used to guide the movements to the target and/or start location. That is, the weights for the RETURN and CORRECTIVE models are adjusted twice on each trial, once based on the outbound error and a second time based on the return movement error. The inclusion of this second error term led to very different patterns of generalization compared with those observed for the ENDPOINT and ONLINE groups (Fig. 7). In particular, for the 180° direction, the trajectory was now shifted in the same rotational direction as at the training location. Note that the effect of this second error term counteracts the direction of generalization induced by the positive baseline activity.

For the CORRECTIVE and RETURN conditions, we had to specify the direction of the corrective movement ($\theta_n^{\text{corrective}}$). The best fit for both groups arises when the planned direction at the time of the second error update is 180°. When other directions were considered, such as −90° and −135°, the fits of the generalization curves for other directions of the corrective movement were much poorer [e.g.,−180°: root mean square error (RMS) = 1.99; −90°: RMS = 2.12; −135°: RMS = 2.91]. The 180° direction seems reasonable for the RETURN group, since these participants must move in this general direction to return to the start location. It is more surprising that 180° value also provides the best fit for the CORRECTIVE group, since movements in this direction would only occur when the participants overshot the target. Participants in the CORRECTIVE group did overshoot early in rotation training, with the mean amplitude 0.8 ± 0.02 cm beyond the target during the first eight reaches to the training location. This tendency decreased over the course of training, with the mean overshoot only 0.07 ± 0.006 cm over the last eight movements of rotation training (t_9 = 5.50, $P < 0.001$).

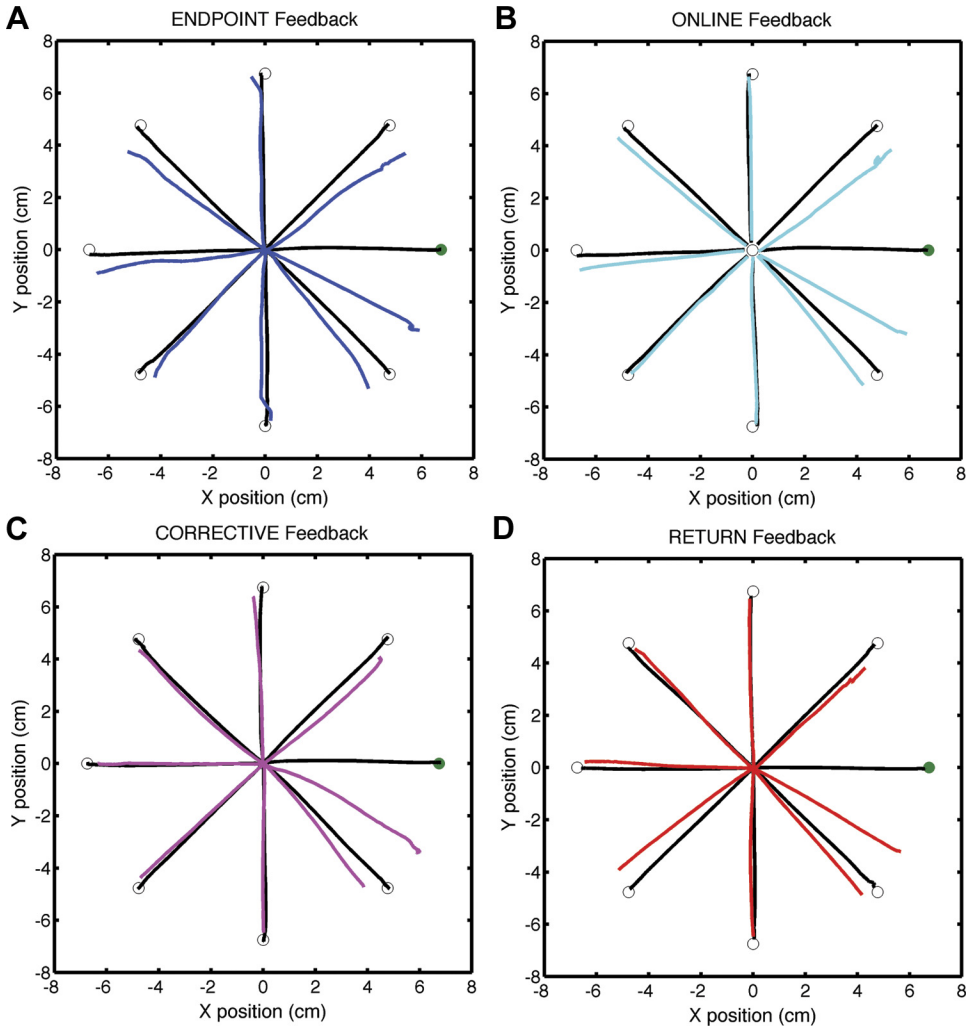

Fig. 5. Hand trajectories during the baseline block (black) and the first cycle of the no-feedback block for the 4 groups: ENDPOINT (blue, *A*), ONLINE (cyan, *B*), CORRECTIVE (purple, *C*), RETURN (red, *D*). Movements were made to all 8 locations without feedback.

We allowed the model to estimate separate learning rates for the second error signal for the RETURN and CORRECTIVE groups given that these error signals were used for different purposes. Three points are of note here. First, the learning rates for the second error signal are considerably smaller than the learning rate for the outbound error signal, presumably reflecting the fact that the compensation for the rotation is based on an error associated with the initial heading direction. Second, the estimated learning rate for the RETURN group is larger than that estimated for the CORRECTIVE group, perhaps because of the large error that occurs when the heading for the return movement is again perturbed by the rotation. Third, the inclusion of separate learning rates for the second error signal provided a much better fit of the generalization function. Overall, the full five-parameter model provides an excellent fit of the generalization function for these groups (Fig. 8; Table 2), accounting for 61% of the unexplained variance from the fit obtained with a simpler three-parameter model (from $r^2 = 0.89$ to 0.96 in the CORRECTIVE condition and from 0.89 to 0.93 in the RETURN condition).

Experiment 2

A central feature of the model is that the current error information is used to modify the synaptic weights of the network elements in a manner proportional to the level of activity of the directionally tuned units that are active at the time of the update. When the movement is made with endpoint-only feedback, only units tuned to the direction of the target are significantly activated, and thus error-based training is specific to those units. However, when corrective movements are made, or when feedback is provided when the participant returns to the start location, units tuned in other directions can be active, resulting in training in those directions leading to what would be measured as a change in generalization. Thus the pattern of generalization will depend on the range of units that are activated when feedback is available.

This architecture predicts that the generalization function should be modified if the set of training locations is increased. Moreover, the form of this function should be modified in a specific manner. Consider a condition in which the training set includes two locations, 0° and −45°, and feedback is provided on the outbound and return movements. Adaptation not only should be observed for movements around these two training locations but also should be evident during generalization for movements to targets at 180° and 135°, the movement directions that are required to return to the start location.

We simulated this two-training target condition, using the model parameters for the RETURN condition from *experiment 1*. During the training block, the model used outbound errors generated for reaches to the 0° and −45° target locations and

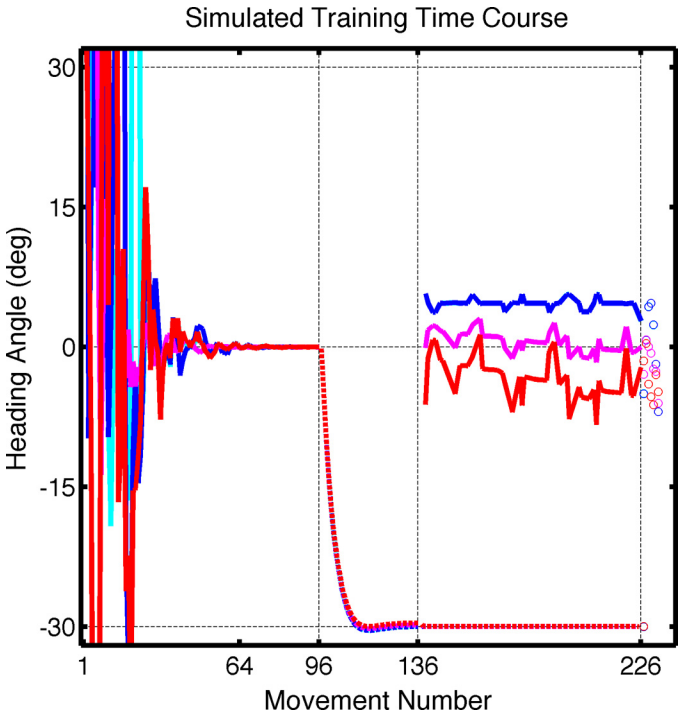

Fig. 6. Model simulation of training in each feedback condition. The weights were initially randomized and the model learned to reach to each target with feedback in the baseline block. During the rotation block, the model learned to compensate for the rotation (3 colored dashed lines are superimposed). Probe targets (colored solid lines) were introduced during the test block (*movements 137–226*). No-feedback block (open circles) was limited to 8 movements (1 per target) since the model was now stable, given the absence of feedback. Blue, ENDPOINT; cyan, ONLINE; purple, CORRECTIVE; red, RETURN. Note that the ENDPOINT and ONLINE groups overlap completely after the training block.

return errors for reaches toward the start location, movements that involved trajectories that corresponded to those required for reaches in the direction of the 180° and 135° targets. The model readily adapted to both training locations. Importantly, the model showed similar generalization around the 180° target and the 135° target (Fig. 9*A*). Thus not only is the spread of generalization larger when there are two targets compared with training at only a single target (Fig. 9*A*), but the form of generalization was in a specific manner for targets distant to the training locations. To confirm that this change in the generalization function was not simply due to training at two locations, we simulated a two-target condition in which feedback was only given at the endpoint of the outbound movement, using here the model parameters from the ENDPOINT condition of *experiment 1*. For this simulation, the model predicted a very different pattern of generalization, similar to that predicted when only one training target is used (Fig. 9*B*).

To empirically test this prediction, we recruited two more groups of participants who were presented with targets at two locations during the rotation phase. One group was provided with continuous online feedback during both the outbound movement and the return (RETURN-TWO group), whereas the other group only received feedback at the end of the reach (ENDPOINT-TWO group), Both groups adapted to the rotation at both training locations (Fig. 10*A*). However, they exhibited very different patterns of generalization during the test block (Fig. 10, *B* and *C*). The RETURN-TWO group showed generalization in the clockwise direction (rotational reference frame), and the magnitude of this effect at the 135° location is larger than that observed for the RETURN group from *experiment 1* (Fig. 10*B*; $t_{18} = 3.10$, $P = 0.006$). In contrast, the ENDPOINT-TWO group showed generalization that was similar to that observed in the ENDPOINT group from *experiment 1* (compare Fig. 3*A* and Fig. 10*C*). In particular, the generalization at the probe locations was in the CCW direction (or downward). No differences were observed between the ENDPOINT-TWO (*experiment 2*) and ENDPOINT (*experiment 1*) conditions in a between-experiment comparison ($t_{18} = 0.62$, $P = 0.55$). In summary, the observed results closely conform to the predictions of the model.

DISCUSSION

In previous studies of visuomotor rotation, generalization has been found to be in the same angular direction of the rotation, leading to the idea that participants develop an internal model of the perturbation (Krakauer et al. 2000; Pine et al. 1996). In the present study, we find that the shape of the generalization function is strongly influenced by the type of visual feedback provided during adaptation. When participants were required to make online corrections to terminate the movement within the target (and during a return movement to the starting location), the pattern of generalization near the training location and at far locations was consistent with the hypothesis that participants had indeed learned a rotational transformation. However, the generalization function was not monotonic, with minimal evidence of learning at directions orthogonal to the training location. Even more striking, when online corrections were not required the angular direction of the generalization function was reversed: Heading errors at these locations were in the opposite direction of the rotation, a pattern consistent with generalization in an exocentric reference frame. These different task demands yielded subtle yet important differences, leading us to reconsider the processes that drive generalization.

We were able to capture these discrepant patterns of generalization in a unified model that emphasizes the important contribution of error information for adjusting the output of movement units defined by a radial basis function network (Tanaka et al. 2009; Thoroughman and Shadmehr 2000; Thoroughman and Taylor 2005). Generalization was defined by three components: *1*) the neural tuning width, *2*) neural baseline activity, and *3*) the error signals experienced by the system during adaptation (Fig. 11). In previous computational studies of generalization, the focus has been on the first two factors that define the shape of the tuning function. Different patterns of generalization observed across several task domains (e.g., rotations, translations, gain changes) have been attributed to differences in the shape of the tuning functions (Ghahramani et al. 1996; Pearson et al. 2010; Tanaka et al. 2009; Thoroughman and Taylor 2005). We find that careful consideration of the error signal is sufficient to account for qualitative changes in generalization without requiring variation in the shape of the tuning function. Indeed, applying a consistent set of principles across task conditions can yield different patterns of generalization from a uniform set of tuning functions, a desirable feature given that the basic task—adaptation of a sensorimotor map—remains constant. Thus differences in generalization

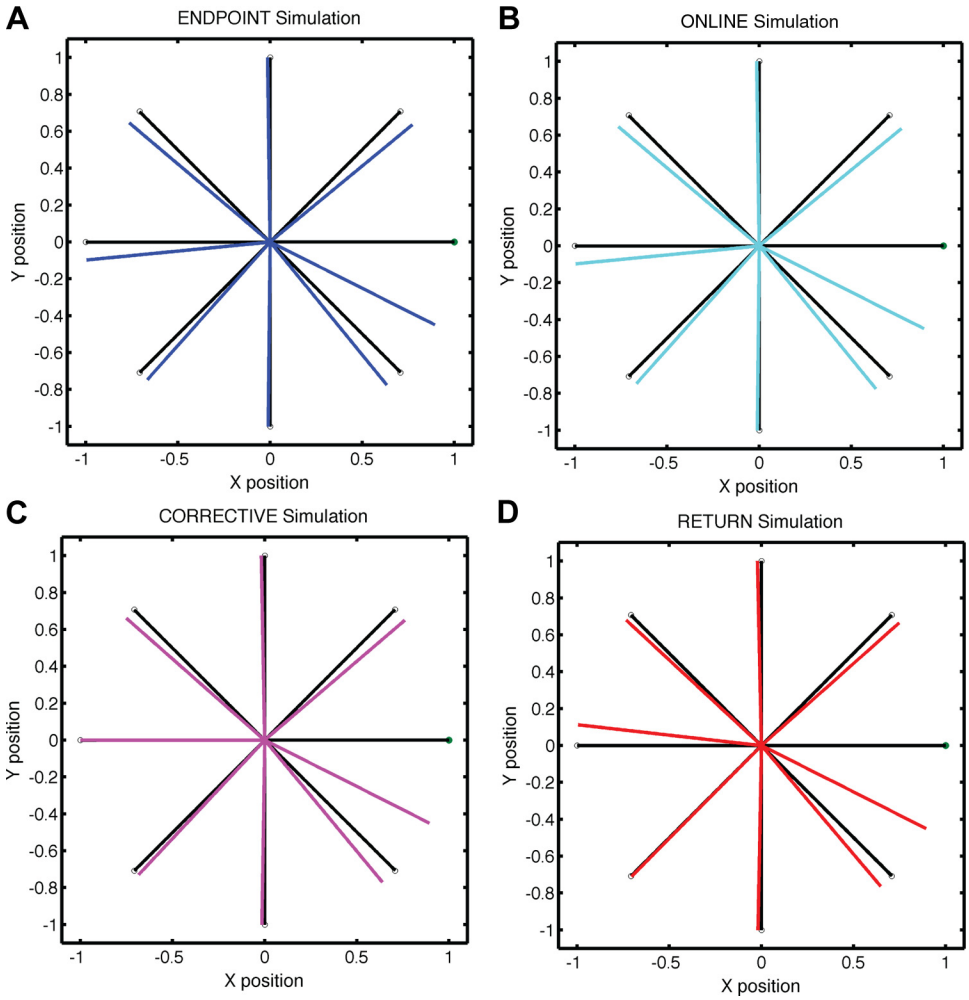

Fig. 7. Model simulation of hand trajectories during the baseline block (black) and no-feedback block for the 4 groups: ENDPOINT (blue, *A*), ONLINE (cyan, *B*), CORRECTIVE (purple, *C*), RETURN (red, *D*).

need not be attributed to differences in the neural representation per se, but rather reflect constraints imposed by the available error information.

Recent work by Brayanov and Smith (Brayanov et al. 2011) has suggested that generalization functions reflect the composite operation of two processes. One process is local in nature, limited to directions similar to the training direction(s), and is manifested in a Cartesian reference frame. The second process is global, affecting all directions, and is manifested in a rotational reference frame. This two-process model is at odds with our model in that we postulate a single process, one in which the units code movement direction in a rotational space but receive an error that is based in a Cartesian reference frame. However, as emphasized in the present study, it is important to consider the type of feedback presented during the training phase. Brayanov and Smith (Brayanov et al. 2011) provided online feedback throughout the movement, requiring the cursor to land in the target region. This form of feedback will provide error information at multiple states, depending on the duration of the movement. This is similar to our CORRECTIVE group (or our RETURN group), where we see either no generalization or rotational generalization at targets far from training. Any differences in our CORRECTIVE group and the work by Brayanov and Smith (Brayanov et al. 2011) could be due to differences in the speed of movements, the time allowed for online corrections, and how generalization is tested during training. Participants receive error feedback at many states (positions) during the corrective feedback portion of the movement, and, according to our model, these additional states during this period also contribute to learning, thereby leading to differences in generalization. Thus any test of generalization may be contaminated by error-based feedback if it is available during training. The pattern of generalization will be different depending on the number of states that are visited and the duration of the reach that involves traveling through states that are not directed toward the target.

Tuning Functions Limit Degree of Generalization

Prior studies have generally observed relatively narrow generalization functions. Substantial generalization is observed near the direction of training, and falls off rapidly as the direction of probe movements deviates from the training direction (Krakauer et al. 2000; Tanaka et al. 2009). The shape of this generalization function has been attributed to the shape of neuronal tuning functions in a radial basis function network (Thoroughman and Shadmehr 2000). These functions can be approximated by a Gaussian, tuned to movement velocity (or direction). The output of the network is the weighted sum of these velocity-tuned units, the population vector (Georgopoulos et al. 1986). When a perturbation is introduced, the weights are adjusted based on an error signal defined by the difference

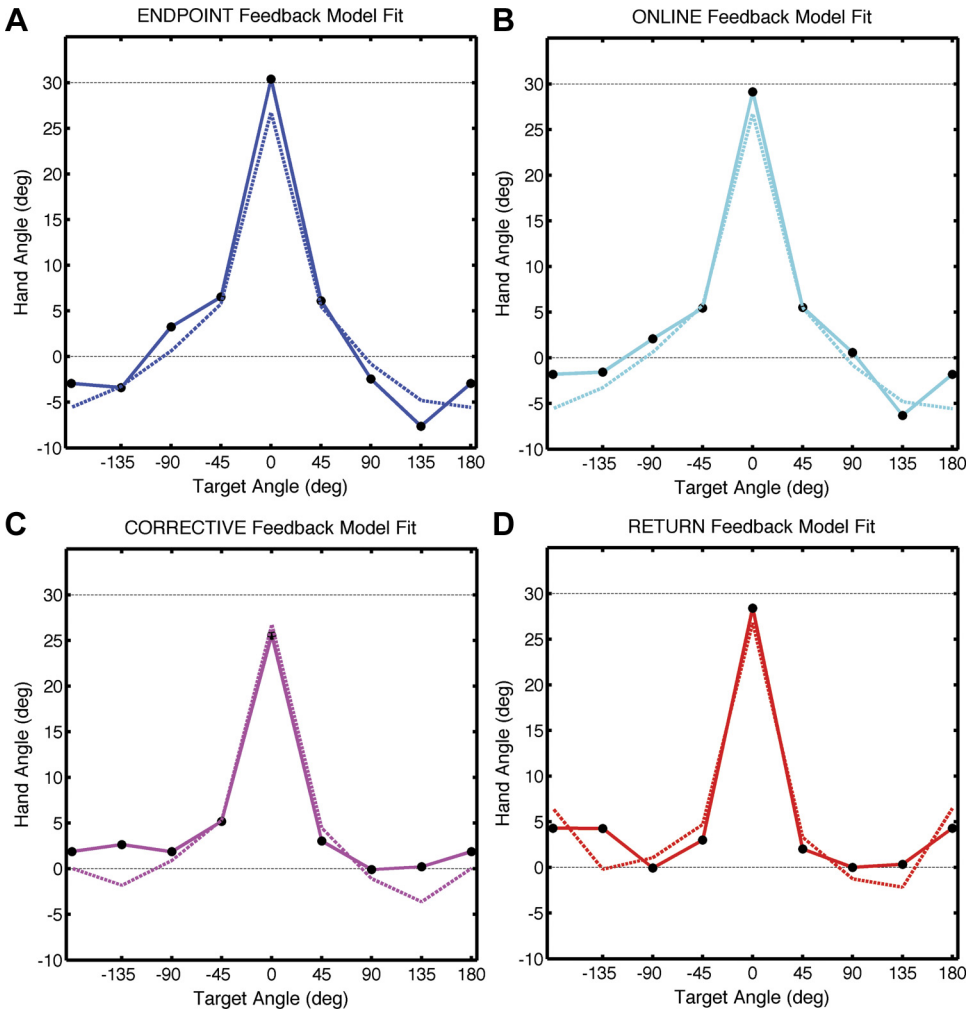

Fig. 8. Model fit of generalization function: average heading angle of the hand at each target location (black circles and solid lines) for each group and the model's heading angle (dashed line). *A*: EF group (blue). *B*: OF group (cyan). *C*: CF group (purple). *D*: RF group (red).

between the planned and observed direction of movement. Stable performance is achieved with a gradient-descent learning rule in which the weights are adjusted proportionally to the size of the error and the unit's level of activity.

In such models, the extent of generalization is constrained by the standard deviation or width of the Gaussian function (Fig. 11). Thus weight adjustments are limited to units that were active during the movement. If the width of the Gaussian function is large, more units will be active for any given movement and, as a consequence, generalization will be broad. If the width of the Gaussian function is small, only a few units are active during each movement and generalization is narrow.

Previous studies have suggested that the widths of the tuning functions are relatively narrow, with estimates ranging from 20° to 30° (Tanaka et al. 2009; Thoroughman and Shadmehr 2000). These estimates suggest that generalization should be of limited extent. While the generalization function does fall off rather sharply from the training direction (e.g., 50% reduction at angles $> 20°$), most studies have also observed some degree of generalization at directions far from the training location (Krakauer et al. 2000; Pine et al. 1996; Tanaka et al. 2009). One proposal to account for distant generalization involves the use of more complicated tuning functions such as a cosine-tuned function or one involving a difference of Gaussians (Thoroughman and Taylor 2005). Functions such as these have been identified in the motor cortex (Georgopoulos et al. 1982), cerebellum (Coltz et al. 1999), and visual cortex (Hubel and Wiesel 1959). An alternative hypothesis is that different subpopulations of neurons have different tuning functions and during learning error signals are used to select the appropriate subpopulations (Thoroughman and Taylor 2005). Both of these hypotheses require sophisticated neural circuitry for tuning selection, and, to date, empirical support for such a learning process has not been identified. While there is evidence of experience-dependent changes in the preferred direction of motor cortex cells (Gandolfo et al. 2000; Paz and Vaadia 2004; Taylor et al. 2002), consistent changes to the shape of the tuning function have not been identified.

Baseline Activity Produces Weak, but Broad, Generalization

We opted to take a different approach here. We assumed that the units could be represented as directionally tuned Gaussian functions with a fixed tuning width (Tanaka et al. 2009). As noted above, this model easily captures the fact that generalization is largest around the trained direction. In addition, we found that a parameter representing (nonzero) baseline neural activity was sufficient to produce a modicum of generalization at distant locations (Ingram et al. 2011; Thoroughman and Taylor 2005). Importantly, this baseline activity does not predict generalization in a rotational frame of reference, but rather in a direction consistent with a Cartesian representation

Table 2. *Parameter estimates and model fits for each group based on the basis function model (Eqs. 1–9)*

		RMS	r^2
Model parameters			
a	0.04		
σ, °	16		
$\eta_{outbound}$	0.18		
$\eta_{corrective}$	0.0007		
η_{return}	0.0017		
$\theta_{corrective}$, °	180		
θ_{return}, °	180		
Model fit			
ENDPOINT		1.68	0.98
ONLINE		1.50	0.98
CORRECTIVE		1.99	0.96
RETURN		2.40	0.93

a, Baseline neural activity; σ, width of the basis function; $\eta_{outbound}$, learning rate for the outbound portion of the movement, constrained to be identical for all 4 groups; $\eta_{corrective}$ and $\theta_{corrective}$, learning rate and desired angle of movement for the corrective portion of the movement for the CORRECTIVE group; η_{return} and θ_{return}, learning rate and desired angle of movement for the return portion of the movement for the RETURN group. Fits were quantified by 2 measures, root mean square error (RMS) and the correlation coefficient (r^2) between the model simulation and group-averaged heading angle during the no-feedback block.

of the error. The presence of baseline activity was critical in reproducing the generalization patterns observed for the ENDPOINT and ONLINE groups.

It is unclear whether baseline activity should be considered a feature of the tuning functions of the neurons or a distinct, separate process. It is possible that the generalization effects at distant locations reflect the operation of a second learning process. That is, the generalization function may be the composite of locally adapted basis tuning functions and a second generic, albeit weaker, process that is applied to all units (Pearson et al. 2010). This generic process may reflect the effects of learning at a more abstract level such as an adjustment in a motor plan (Fig. 11). For example, after seeing that movements to the training location consistently result in an upward error, the participant may be biased to move in the downward direction, a bias that could be broadcast uniformly across all movement directions.

The baseline parameter was fixed for all four groups. While the model with this term was sufficient to account for generalization in the ENDPOINT and ONLINE groups, it failed to provide an adequate fit for the CORRECTIVE and RETURN groups. For these groups, generalization was either minimal at all distant locations or in a direction consistent with the rotation. If the baseline activity were the sole source of the distant generalization, it would be necessary to postulate that baseline activity is influenced by the task demands. As an intrinsic feature of the tuning functions, the baseline activity would have to be subject to some form of experience-dependent plasticity to account for the group differences. Alternatively, if the baseline activity represented a separate process that provided a generic error signal, we would have to propose that this signal varied between groups. This seems unlikely, given that all of the groups were trained with the same target and showed very similar adaptation at this location.

Importance of Error Signals During Training

To account for the group differences in generalization, we explored the influence of error information, a feature of the model that builds naturally on the different task demands imposed on the four groups. As in standard models of adaptation, the units in our model were updated by an error signal, representing the difference between the desired and actual movement. However, the task demands were more stringent for the CORRECTIVE and RETURN groups. For the former, the movement had to terminate in the target location; for the latter, feedback was also available when the participant returned to the start position. The feedback available to guide these corrections not only provides a source of additional error information but also is utilized at a time when the dynamics of the network has changed: The pattern of activation across the units in the neural network is altered and, as such, has altered the landscape in terms of which units are eligible for updating. We modeled this by introducing a second error-updating epoch for these two groups. The inclusion of this additional error term was capable of generating the generalization curves exhibited by the CORRECTIVE and RETURN groups. The parameter estimates suggest that the error information used for the second update is not as salient for the CORRECTIVE condition compared with the RETURN condition. Note that this difference is how the model accounts for the difference in generalization between the two groups; as such, it cannot be said to be

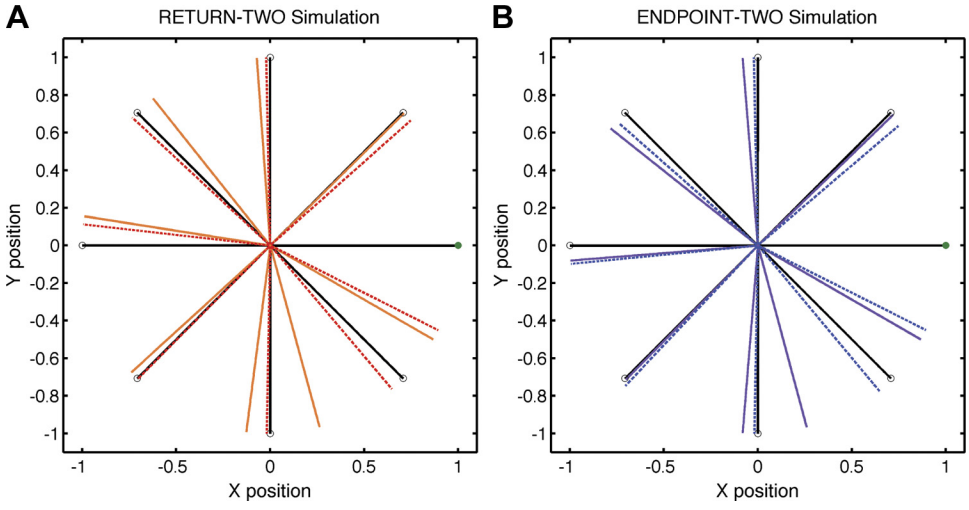

Fig. 9. Predicted hand trajectories from the model during the baseline block (black) and no-feedback block for conditions in which 2 targets are used during the training block with either online feedback during the outbound and return phases (RETURN-TWO, orange; *A*) or endpoint-only feedback (ENDPOINT-TWO, purple; *B*). The predictions were derived by using parameters estimated from the data fits for *experiment 1* when only 1 target had been used during training.

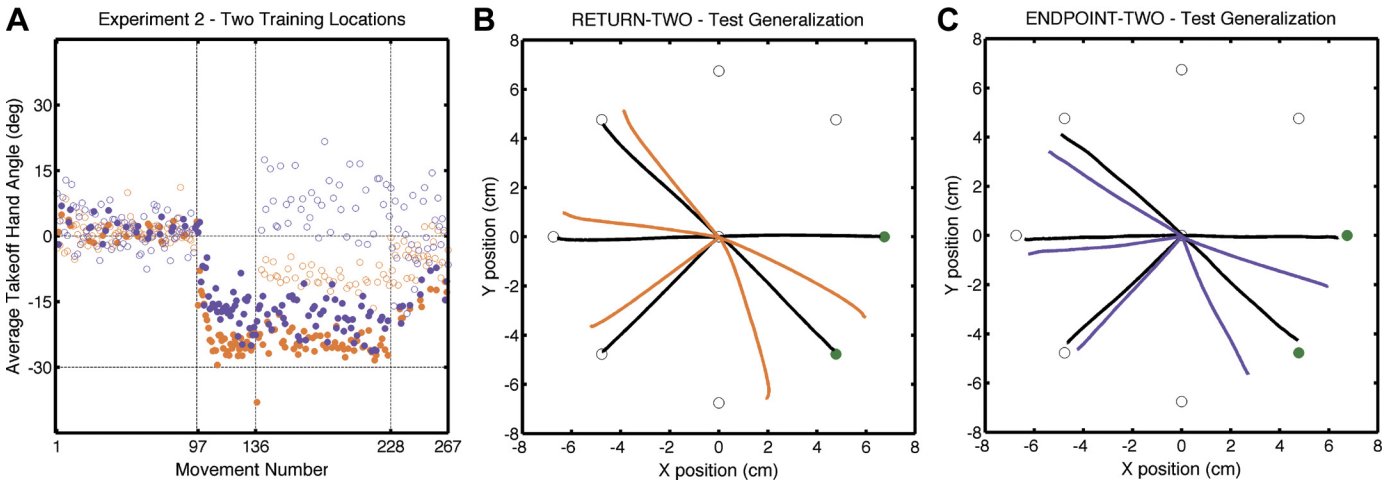

Fig. 10. *A*: heading angle relative to target direction during baseline (*trials 1–96*), rotation (*97–136*), test (*137–227*), and no-feedback (*228–266*) blocks. The ENDPOINT-TWO group is in blue and the RETURN-TWO group in orange. Movements to the training target location are filled circles, and movements to the other locations are open circles. *B* and *C*: RETURN-TWO group (*B*) and ENDPOINT-TWO group (*C*) hand trajectories during the baseline block (black) and test block. As in *experiment 1*, feedback was only provided when the target appeared at the 2 training locations (green) in the test block.

an "explanation." Nonetheless, the model clearly demonstrates how generalization is influenced by the form of the error information.

We recognize that our discrete use of feedback information is a simplification. Differences between the observed and simulated data, especially for the return condition, may be due to undersampling of the error signal given that we limited the updating process to two time points. We expect that the fits would improve if we used more time points. While error information is continuously available, it remains to be seen whether updates to the motor commands are provided in a continuous or discrete manner (Flash and Henis 1991; Ijspeert et al. 2002). The point we wish to emphasize here is that the inclusion of error signals that conform to the basic task demands was sufficient to produce qualitatively different generalization functions. For all four groups, the outbound error adjustment was based on an error defined by the initial heading direction (measured between 1 and 3 cm; see MATERIALS AND METHODS). For the CORRECTIVE and RETURN groups, the second error adjustment was applied when the movement was heading in the reverse direction (180°, based on the model fits). We were surprised to find that the best fit for the CORRECTIVE group was obtained when the second error adjustment was applied to units generating trajectories in the 180° direction. A priori, we expected that, given the rotation, the 90° or 135° directions would be more relevant for this group. If the second error term had updated units producing trajectories in these directions, then significant generalization should have been observed for reaches to targets at these directions, a result that was not present in the participants' generalization curves. It is possible that the return movement, with its prominent 180° direction, is especially salient given the need to return to the center location before the next trial. This may produce a greater emphasis on this direction for error updating. Alternatively, error information may be delayed with respect to the units that were responsible for the errors. If this information was not properly maintained in memory, then the system could misapply the error information. Thus recent errors in a particular direction may be used to update units specifying the current direction, resulting in the wrong errors being applied to the wrong units.

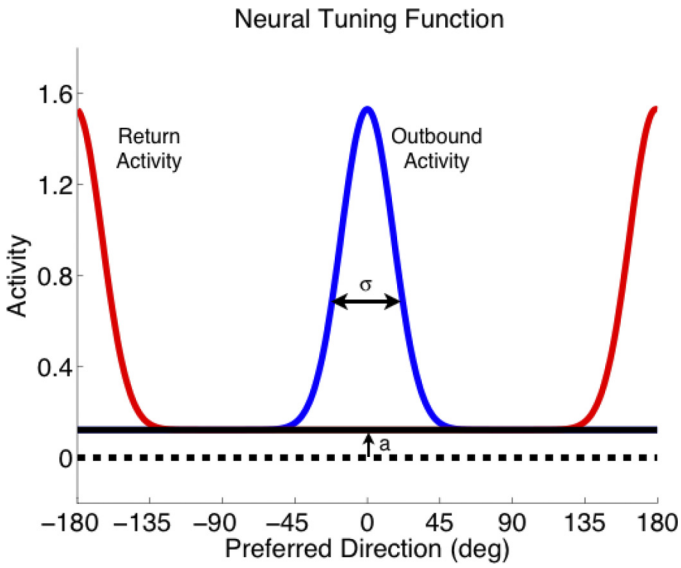

Fig. 11. Schematic activity level of directionally tuned units during the outbound (blue) and return (red) phases of a movement to the training target (0°). The generalization function is determined by 3 components: baseline activity (*a*), tuning width (σ), and modification of the weights determining the contribution of each unit to the population vector. These weights are updated based on an error signal generated during the outbound phase of the movement for all groups and the return phase for the CORRECTIVE and RETURN groups.

Nevertheless, the present data fits and simulations show that using just two error updates, one for the outbound phase and a second for the return phase, can lead to qualitative changes in the generalization function. This point is underscored by the results of *experiment 2*, where we observed a change in the generalization at specific locations, distant from the training locations. Thus a simplified model in which the utilization of error information is likely sparser than in reality was sufficient to predict the general shape of generalization functions; we assume that a more realistic model would provide even better quantitative fits to bolster these qualitative observations. An important implication of our work is that it may be a misnomer to refer to the trajectory changes for movements to probe

locations as "generalization," at least for the RETURN groups. Generalization implies that a behavioral change is the result of learning a particular task or movement. As the modeling work presented here makes clear, the behavioral changes at probe locations for the RETURN group are the result of a directed movement toward the starting location. Prior studies of generalization have tended to use tasks in which visual feedback was continuously available. As shown here, generalization in these studies is "contaminated" by the utilization of error information during both the outbound and return phases of the movements. Most importantly, the modeling work makes clear that we need not assume different representations to account for task-dependent differences in generalization. Rather, a parsimonious account of these differences is possible when consideration is given to the error information available during learning.

ACKNOWLEDGMENTS

We are grateful to Maurice Smith and Jordan Brayanov for their many comments throughout the course of this project. We thank Christina Gee for help with data collection and Jon Berliner for help with manuscript preparation.

GRANTS

J. A. Taylor was supported by an National Research Service Award fellowship (F32-NS-064749) from the National Institute of Neurological Disorders and Stroke, and R. B. Ivry was supported by Grant 5R01-HD-060306 from the National Institute of Child Health and Human Development.

DISCLOSURES

No conflicts of interest, financial or otherwise, are declared by the author(s).

AUTHOR CONTRIBUTIONS

Author contributions: J.A.T. and R.B.I. conception and design of research; J.A.T. and L.L.H. performed experiments; J.A.T. analyzed data; J.A.T., L.L.H., and R.B.I. interpreted results of experiments; J.A.T. prepared figures; J.A.T. drafted manuscript; J.A.T., L.L.H., and R.B.I. edited and revised manuscript; J.A.T., L.L.H., and R.B.I. approved final version of manuscript.

REFERENCES

Brayanov JB, Petreska B, Smith M. Visuomotor transformations elicit simultaneous learning in two distinct coordinate systems. *Neuroscience Meeting Planner*. Washington, DC: Society for Neuroscience, program no. 387.27, 2011.

Coltz JD, Johnson MT, Ebner TJ. Cerebellar Purkinje cell simple spike discharge encodes movement velocity in primates during visuomotor arm tracking. *J Neurosci* 19: 1782–1803, 1999.

Donchin O, Francis JT, Shadmehr R. Quantifying generalization from trial-by-trial behavior of adaptive systems that learn with basis functions: theory and experiments in human motor control. *J Neurosci* 23: 9032–9045, 2003.

Flash T, Henis E. Arm trajectory modification during reaching towards visual targets. *J Cogn Neurosci* 3: 220–230, 1991.

Gandolfo F, Li C, Benda BJ, Padoa Schioppa C, Bizzi E. Cortical correlates of learning in monkeys adapting to a new dynamical environment. *Proc Natl Acad Sci USA* 97: 2259–2263, 2000.

Georgopoulos AP, Kalaska JF, Caminiti R, Massey JT. On the relations between the direction of two-dimensional arm movements and cell discharge in primate motor cortex. *J Neurosci* 2: 1527–1537, 1982.

Georgopoulos AP, Schwartz AB, Kettner RE. Neuronal population coding of movement direction. *Science* 233: 1416–1419, 1986.

Ghahramani Z, Wolpert DM, Jordan MI. Generalization to local remappings of the visuomotor coordinate transformation. *J Neurosci* 16: 7085–7096, 1996.

Hinder MR, Tresilian JR, Riek S, Carson RG. The contribution of visual feedback to visuomotor adaptation: how much and when? *Brain Res* 1197: 123–134, 2008.

Hubel DH, Wiesel TN. Receptive fields of single neurones in the cat's striate cortex. *J Physiol* 148: 574–591, 1959.

Ijspeert AJ, Nakanishi J, Schaal S. Movement imitation with nonlinear dynamical systems in humanoid robots. *IEEE International Conference on Robotics and Automation*, 2002, p. 1398–1403.

Ingram JN, Howard IS, Flanagan JR, Wolpert DM. A single-rate context-dependent learning process underlies rapid adaptation to familiar object dynamics. *PLoS Comput Biol* 7: e1002196, 2011.

Izawa J, Shadmehr R. Learning from sensory and reward prediction errors during motor adaptation. *PLoS Comput Biol* 7: e1002012, 2011.

Krakauer JW, Pine ZM, Ghilardi MF, Ghez C. Learning of visuomotor transformations for vectorial planning of reaching trajectories. *J Neurosci* 20: 8916–8924, 2000.

Nelder JA, Mead R. A simplex method for function minimization. *Computer J* 7: 308–313, 1965.

Oldfield RC. The assessment and analysis of handedness: the Edinburgh inventory. *Neuropsychologia* 9: 97–113, 1971.

Paz R, Vaadia E. Learning-induced improvement in encoding and decoding of specific movement directions by neurons in the primary motor cortex. *PLoS Biol* 2: E45, 2004.

Pearson TS, Krakauer JW, Mazzoni P. Learning not to generalize: modular adaptation of visuomotor gain. *J Neurophysiol* 103: 2938–2952, 2010.

Pine ZM, Krakauer JW, et al. Learning of scaling factors and reference axes for reaching movements. *Neuroreport* 7: 2357–2361, 1996.

Poggio T, Bizzi E. Generalization in vision and motor control. *Nature* 431: 768–774, 2004.

Pouget A, Snyder LH. Computational approaches to sensorimotor transformations. *Nat Neurosci* 3, *Suppl*: 1192–1198, 2000.

Rapp K, Heuer H. Active error corrections enhance adaptation to a visuomotor rotation. *Exp Brain Res* 211: 97–108, 2011.

Savitzky AG, Golay MJ. Smoothing and differentiation of data by simplified least squares procedures. *Anal Chem* 36: 1627–1639, 1964.

Shabbott BA, Sainburg RL. Learning a visuomotor rotation: simultaneous visual and proprioceptive information is crucial for visuomotor remapping. *Exp Brain Res* 203: 75–87, 2010.

Smith MA, Brandt J, Shadmehr R. Motor disorder in Huntington's disease begins as a dysfunction in error feedback control. *Nature* 403: 544–549, 2000.

Tanaka H, Sejnowski TJ, Krakauer JW. Adaptation to visuomotor rotation through interaction between posterior parietal and motor cortical areas. *J Neurophysiol* 102: 2921–2932, 2009.

Taylor DM, Tillery SI, Schwartz AB. Direct cortical control of 3D neuroprosthetic devices. *Science* 296: 1829–1832, 2002.

Thoroughman KA, Shadmehr R. Learning of action through adaptive combination of motor primitives. *Nature* 407: 742–747, 2000.

Thoroughman KA, Taylor JA. Rapid reshaping of human motor generalization. *J Neurosci* 25: 8948–8953, 2005.

Tseng YW, Diedrichsen J, Krakauer JW, Shadmehr R, Bastian AJ. Sensory prediction errors drive cerebellum-dependent adaptation of reaching. *J Neurophysiol* 98: 54–62, 2007.

Vindras P, Viviani P. Altering the visuomotor gain. Evidence that motor plans deal with vector quantities. *Exp Brain Res* 147: 280–295, 2002.